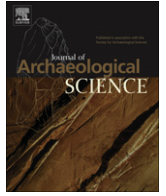


Contents lists available at [SciVerse ScienceDirect](http://www.elsevier.com/locate/jas)

Journal of Archaeological Science

journal homepage: <http://www.elsevier.com/locate/jas>

Environmental changes in the Maryut lagoon (northwestern Nile delta) during the last ~2000 years

Clément Flaux^{a,*}, Mena El-Assal^b, Nick Marriner^a, Christophe Morhange^a, Jean-Marie Rouchy^c, Ingeborg Soulié-Märsche^d, Magdy Torab^b

^a CEREGE CNRS UMR 6635, Université Aix-Marseille, Europôle de l'Arbois, BP 80, 13545 Aix-en-Provence cedex 04, France

^b Alexandria University, Department of Geography, Damanhour Branch, Egypt

^c Département Histoire de la Terre, Muséum National d'Histoire Naturelle, 43 rue Buffon, 75005 Paris, France

^d Institut des Sciences de l'Evolution, UMR 5554 du CNRS, Université Montpellier 2, C.P. 061, Place E. Bataillon F, 34095 Montpellier-Cedex 5, France

ARTICLE INFO

Article history:

Received 9 July 2011

Received in revised form

13 June 2012

Accepted 15 June 2012

Keywords:

Alexandria

Lake Mareotis

Nile

Holocene

Coastal geomorphology

Bio-sedimentology

Palaeoenvironment

Human impacts

Geoarchaeology

ABSTRACT

Here, we interpret the evolution of Maryut lagoon (Egypt) during the past ~2000 years. Chronostratigraphy and laboratory analyses have enabled us to identify four main phases since the 3rd century AD: (1) a fluvial-dominated lagoon between the 2nd–3rd and the 8–9th centuries cal. AD; (2) a gradual desiccation of the lagoon toward a sebkha-like environment from the 9–10th to the 13th centuries cal. AD; (3) a fluvial-dominated lagoon from the 13th century cal. AD; and (4) a second gradual desiccation between the 17th and the 18th centuries cal. AD. The general aridification trend described throughout the study period may be linked to the gradual decline of the Canopic branch, which supplied the Maryut lagoon with freshwater. Nonetheless, at shorter timescales, the different phases of lagoon aridification and flooding coincide with land abandonment and irrigation works in the region. It is suggested that the history of the Alexandria countryside has been a key driver in shaping the environmental history of the Maryut during the past ~2000 years.

© 2012 Elsevier Ltd. All rights reserved.

1. Introduction

During antiquity, the Maryut lagoon served as a navigation channel for the transportation of goods and passengers between Alexandria, its agricultural hinterland and the Nile delta (Cosson (de), 1935; Empereur, 1998; Rodziewicz, 1998; Empereur and Picon, 1998; Khalil, 2005). The shores of the lagoon have been densely occupied since the 4th century BC (Blue and Khalil, 2010; Blue et al., 2011). Land reclamation of the delta's western margin began during the early Ptolemaic period and continued during Roman times, according to historical sources, although the extent of irrigation and drainage works is unknown (Redon, 2007, pp. 450–459). After the Arab conquest, in the 7th century AD, sites at the shoreline declined rapidly and traffic on the Maryut waterway ceased progressively (Décobert, 2002). Nonetheless, cultivated lands in the Behera region, between the Rosetta branch of the Nile and the Maryut lagoon (Fig. 1), were not abandoned during the

Medieval period. This archaeological and historical evidence shows: (1) that the Maryut basin has been a key feature of Alexandria since antiquity; and (2) sheds light on possible human impacts in shaping the lagoon's environmental history, notably its hydrology. Nonetheless, the late Holocene evolution of Maryut lagoon is poorly understood. To fill this knowledge gap, we analyzed the basin's late Holocene environmental history using stratigraphic sequences and bio-sedimentological data. Historical descriptions of the Maryut lagoon by travelers are also used. Our study aims to identify potential human impacts upon the Maryut's environment and, in turn, the role of natural forcing in shaping human occupation patterns in the Alexandria region.

2. Environmental setting

The Maryut lagoon lies on the northwestern edge of the Nile Delta. The lagoon can be subdivided into two parts, the western arm and the main eastern body (Fig. 1). The western area is structured by two late Pleistocene coastal ridges trending SW–NE parallel to the present coastline (Fig. 1; El Asmar and Wood, 2000). The Maryut's eastern body is flanked in the north by

* Corresponding author.

E-mail address: flaux@cerege.fr (C. Flaux).

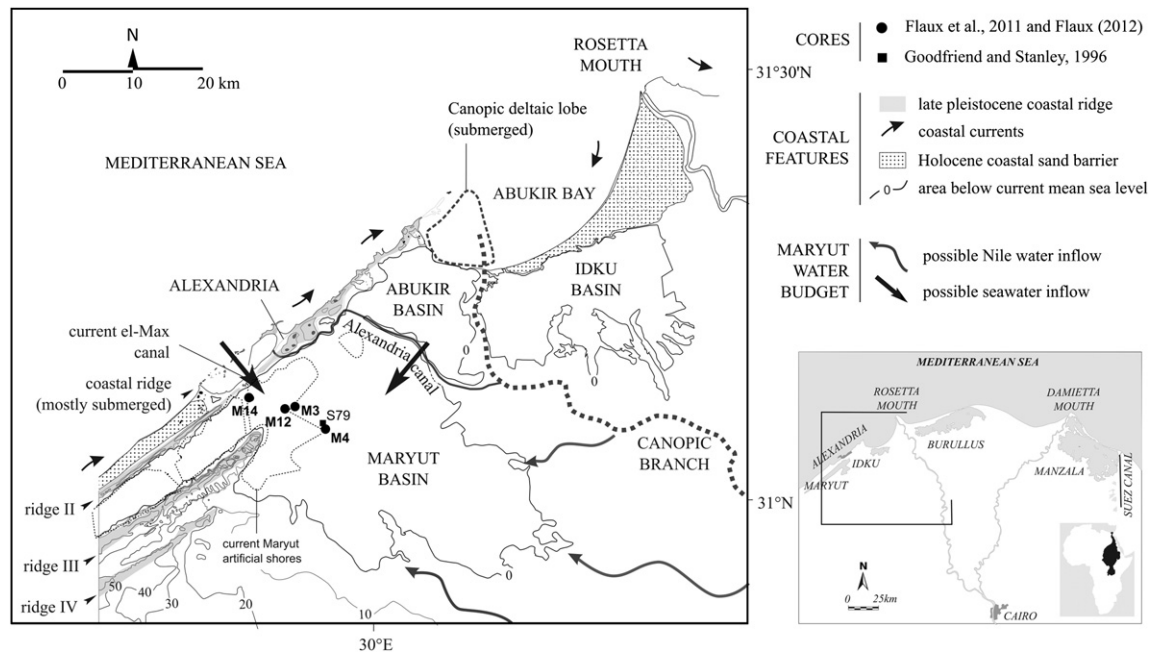


Fig. 1. Main topographical and palaeo-geomorphological features of the northwestern Nile delta. The location of core sites is also shown. Sources: 1/100,000 topographic map of Egypt, sheet 88-42 El-Hammam (1926), sheet 88-48 al-Ghayata (1927), sheet 88-48 Kafr Ez-Zaïet (1927), sheet 92-48 Alexandria (1930), sheet Damanhour 92/54 (1934). Drawn by the Generalstab des Heeres Abteilung für Kriegskunde und Vermessungswesen (Abteilung IV Mil. Geo.). Published by the Survey of Egypt[®] archives; Jana Helmbold; geological map; Quickbird satellite image; field observations; underwater Canopic lobe data after Stanley et al., (2004a, 2004b).

a coastal ridge, in the east by the Mahmoudeya canal (former Alexandria canal) and in the west by Quaternary deposits that overlie the Miocene limestone. In the south, the basin trends parallel to the western delta edge. Maryut's current southern limit is controlled by pumping stations that maintain water levels at 2.8 m below mean sea level (bmsl). As a result, most of the previous Maryut southeastern basin has been reclaimed for agricultural purposes (Fig. 1). The Maryut receives water from the Nile's northwestern delta irrigation system, as well as industrial and urban wastewater from Alexandria (ALAMIM, 2007). As a consequence, salinity is nearly nil to low-brackish.

Human modification of the water budget has a long history in the area. At the end of the 12th century AD, the chronicler Abul Hassan al-Makhzoumi described the irrigation system during Nile flooding of the province of Behera (in Toussoun, 1926), an administrative region located on the northwestern delta, between the Rosetta branch and the Maryut lagoon (Fig. 1). The Behera was divided into several basins separated by dikes. Each basin was flooded successively by opening of the dikes, beginning with the Nile in the west. The excess water leads to flooding of the Maryut basin. Earlier in antiquity, Redon (2007) cites historical documents attesting to drainage works in the area of Maryut lagoon.

In addition to human impacts, natural forcings may also act as drivers of lagoonal change. The Maryut's hydrological system is mainly controlled by (1) relative sea-level rise, which includes subsidence processes well documented on the coastline of Alexandria and Abukir bay (Stanley et al., 2004a; Stanley, 2005; Goiran et al., 2005; Stanley and Toscano, 2009) and (2) variability in Nile flow. The Nile has a seasonal flow regime which results from the monsoon rainfall regime of the Blue Nile that drains the Ethiopian highlands (Woodward et al., 2007). Kondrashov et al. (2005) have demonstrated that decennial to centennial climate variability can also affect Nile flow. In addition, Nile flow on the delta has been subjected to lateral migration. For instance, during antiquity, the Canopic was the most western branch of the Nile delta (Fig. 1). The Maryut, Alexandria and

its agricultural region were dependent upon the Canopic for fresh-water supplies. The branch has gradually silted up since antiquity, while the Rosetta branch in the east became predominant (Toussoun, 1922, 1926; Bernard, 1970; Chen et al., 1992; Stanley et al., 2004b; Stanley and Jorstad, 2006).

3. Materials and methods

3.1. Sedimentology and chronology

The present study is based on 15 stratigraphic sequences, retrieved from cores and sections (Fig. 1). All localities have been benchmarked relative to present mean sea level using a differential GPS. Boreholes M12 and M14 were drilled using a manual auger operating upon artificial banks above current water level. Sections M3 and M4 were outcrops studied on the banks of low-level water drains. Sections were between 1 and 3 m in height. These sequences are located in the deepest part of the basin (Fig. 1) namely the area the most conducive to recording lowstand sedimentation. Sedimentary features were described during fieldwork. One or more samples were taken from each stratigraphic unit. These were subsequently sieved to quantify the sediment texture, and the composition of the sand fraction was observed under a binocular microscope. Particular attention was paid to faunal groups, characeae and gypsum crystals.

The chronological framework of the Maryut sequence was elucidated using thirteen radiocarbon dates (AMS). Material, sample depths and calibrations are reported in Table 1.

3.2. Historical data

Sedimentological data were complemented by historical descriptions of the Maryut lagoon. Sennoune (2008) has compiled numerous accounts written by travelers who visited Alexandria between the 6th and the 18th centuries AD. Descriptions of the

Table 1

AMS radiocarbon ages and calibrated radiocarbon ages of shells and organic matter in core M3, M4, M12 and M14 taken in Maryut lake. No reservoir age correction (discussion in text). Datations were calibrated by using software Calib v. 6.0 (Stuiver et al., 2005) and *Intcal09* calibration curve (Reimer et al., 2009).

Lab code	Core	Material	Depth (m. bmsl)	d13C	Radiocarbon age years B.P.	Cal. age year A.D. 2 σ range
SacA 16150	M3	Connected shells <i>Cerastoderma gl.</i>	3.7	2.70	345 ± 30	1466–1637
SacA 11629	M3	Rich-organic sediment	3.8	–25.20	300 ± 30	1489–1654
SacA 16148	M3	Ostracods shells <i>Cyprideis torosa</i>	3.90–3.94	–3.30	750 ± 30	1222–1286
SacA 16149	M3	Ostracods shells <i>Cyprideis torosa</i>	4.5	–2.60	1790 ± 30	132–330
SacA 11628	M3	Connected shells <i>Cerastoderma gl.</i>	4.72	2.50	3015 ± 30	1131–1385 cal yr BC
SacA 11625	M4	Connected shells <i>Cerastoderma gl.</i>	3.72	2.60	3030 ± 30	1134–1395 cal yr BC
SacA 11626	M4	Connected shells <i>Scrobicularia plana</i>	3.42	–12.60	680 ± 30	1270–1389
SacA 11627	M4	Connected shells <i>Cerastoderma gl.</i>	3.10	–6.40	PMC ^a 120.29 (±0.23)	post 1960 AD
SacA 11656	M4	Amphibious gastropod	3.25	–4.30	PMC ^a 109.10 (±0.21)	post 1960 AD
SacA 11636	M12	Organic matter	2.90	–27.30	250 ± 30	post 1522
SacA 11637	M12	Wood	3.20	–26.60	165 ± 30	post 1662
SacA 11638	M12	Wood	5.10	–13.60	1205 ± 30	694–894
SacA 11652	M14	Rich-organic sediment	4.80	–24.80	950 ± 30	1024–1156

^a ¹⁴C activity in Percent Modern Carbon (PMC).

lagoon are usually short but nonetheless yield insights into the basin size, its connection to the Nile and/or the sea, the surrounding landscape, and its fish or salt resources. Ancient maps, drawn between the 16th and 18th centuries AD, are given in Awad (2010). From these sources, we obtained forty descriptions of the Maryut between the 16th and the 18th centuries AD.

4. Late Holocene chronostratigraphy of the Maryut lagoon

Results from two sections (M3 and M4) and two cores (M12 and M14) are described below. These cores lie on an SE–NW transect, crossing the deepest part of the Maryut.

4.1. Stratigraphy and biofacies of section M3

The location of section M3 is given in Fig. 1. Seven stratigraphic units have been identified (Figs. 2 and 3).

Unit A comprises an alternation of mud layers devoid of fauna and shelly-rich mud layer (Flaux et al., 2011). The biofacies is characterized by lagoonal pelecypods (*Cerastoderma glaucum*, *Scrobicularia plana* and *Loripes lacteus*), gastropods (*Hydrobia* sp., *Pirenella conica*), the foraminifera *Ammonia beccarii* and the ostracod *Cyprideis torosa*. *C. torosa* density exceeds 1000 individuals per 10 g of bulk sediment. The termination of this deposit is dated to 1131–1385 cal. BC, from a shell collected at the top of the unit.

Unit B is characterized by light brown clayey silt rich in *C. torosa*, whose abundance increases to ~40,000 individuals per 10 g of sediment aggregate. This ostracod species constitutes the majority of the medium-size sand fraction (Fig. 3). The associated fauna comprises typical lagoonal species (the foraminifera *A. beccarii*, the pelecypods *C. glaucum* and *S. plana* and the gastropod *Hydrobia* sp.) and slightly brackish water species (the gastropod *Melanoides tuberculata*). The facies also presents sandy lenses, rich in rhizoconcretions (Fig. 4A and B) and the gastropod *Gyraulus* sp. The interface between units B and C is irregular. A radiocarbon date was obtained from ostracod shells taken at the base of the unit. These yielded an age range of 132–330 cal. AD.

Unit C consists of brown clayey silt, mottled with numerous traces of oxidation. *C. torosa* is the only faunal species present, characterized by a sharp decrease in abundance, from >1000 individuals per 10 g of sediment aggregate at the top of unit B to ~10 individuals per 10 g of bulk sediment in this unit (Fig. 3). Gypsum was found in great quantity within the sediment matrix, mainly in discoidal lenticular forms. A white silty sand, also composed of gypsum, was observed in section. This feature formed a mycelium-like system (Fig. 4D) or cylindrical nodules.

Unit D is composed of brown clayey silt. This unit presents the same faunal assemblage as unit B.

Unit E comprises millimetric to centrimetric laminae of sandy gypsum and dark gray muds (see Figs. 3 and 4C). Only a few individuals of *C. torosa* were found in this quasi-azoic environment. Textural analyses indicate that the sand fraction comprises up to 50% in this facies. X-ray analysis of the sand fraction shows that it is primarily composed of gypsum. Crystalline gypsum morphologies are dominated by discoidal lenticular forms. They are associated with tabular and elongated prismatic crystals, with hemi- or bipyramidal endings. Twinned lenticular crystals are frequent, sometimes aggregated to form gypsum flowers. Crystalline overgrowths are also observed on the largest grains. Post-depositional desiccation cracks have altered the structure of the deposit (Fig. 2). They are infilled with sediment from the above unit.

Unit F is a brownish to grayish clayey silt. It presents the same faunal group as unit B. Radiocarbon dating of the base of the unit yielded an age range of 1222–1286 cal. AD.

Unit G consists of dark gray clayey silt. The same faunal groups as unit B are observed. Additional observations include organic-rich lenses, abundant shells of *Hydrobia* sp. and *Gyraulus* sp. in the sandy fraction, amphibious gastropod shells and abundant gypsum in mycelium-like form (Fig. 4D). Gypsum grains are aggregated. The top of the layer lies at the same elevation as the surrounding fields and is covered by embankments. Two ¹⁴C dates indicate that the last sedimentation phase occurred during the 16th to 17th centuries cal. AD.

4.2. Stratigraphy and biofacies of core M12

Core M12 was recovered less than 1 km west of M3 (Fig. 1). Four stratigraphic units have been identified (Fig. 5).

Unit A comprises dark gray muds, rich in lagoonal pelecypod and gastropod shells. It is the same facies as unit A in section M3 (Flaux et al., 2011).

Unit B is a dark brown to black clayey silt, rich in organic matter. Its biofacies consists of lagoonal shells (*A. beccarii*, *C. glaucum*, *S. plana* and *Hydrobia* sp.) and slightly brackish water species (*M. tuberculata*). The abundance of *C. torosa* decreases from units A to B and is accompanied by gypsum formation within the sediment matrix. Two forms of gyrogonites, the calcified fructifications of the Characeae, were identified as *Chara tomentosa* and *Chara zeylanica*. A sample of organic matter taken in this unit yielded an age of 694–894 cal. AD.

Unit C is a gray to dark gray clayey silt, characterized by a decrease in faunal abundance and an increase in gypsum grains. Gypsum grains comprise the majority of the sand fraction. Crystal

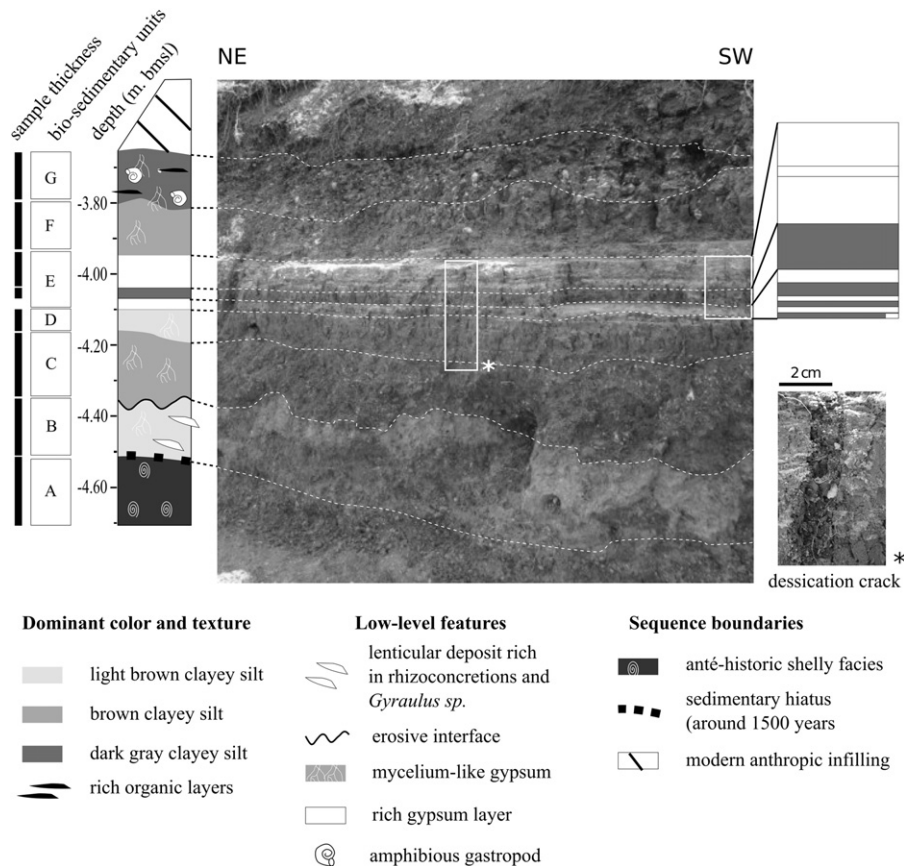


Fig. 2. Stratigraphy of section M3 (location denoted in Fig. 1) and sedimentary features. Upper part of the Maryut lagoon's Holocene sequence.

morphologies are identical to those described in section M3, unit E. Fauna is represented by a few *Hydrobia* sp., *A. beccarii* and *C. torosa*.

Unit D contains *C. glaucum* and *Hydrobia* sp., mixed with gypsum and the hypohaline species *M. tuberculata*. Two dates indicate that this unit was deposited between the 16th and the 20th centuries cal. AD. The uppermost part consists of human infill and forms the embankment of El-Nubareya canal. The latter was dug between 1950 and 1970 (Awad, 2010). It marks the end of the lacustrine sedimentary sequence at site M12.

4.3. Stratigraphy and biofacies of section M4

Section M4 is situated 5 km southeast of point M3 (Fig. 1). Five stratigraphic units have been identified (Fig. 6).

Unit A comprises the same dark shelly mud facies described in M3 and M12. The termination date of this deposit is 1134–1395 cal. BC, from a shell collected at the top of the unit. This date is similar to the one obtained from section M3.

Unit B is a light gray clayey silt. No shells were recorded but some gypsum grains were found within the sediment matrix.

Unit C is a gray to dark gray clayey silt. The fauna comprises lagoonal species (foraminifera *A. beccarii*, ostracod *C. torosa*, gastropod *Hydrobia* sp., pelecypods *C. glaucum* and *S. plana*) and slightly brackish to freshwater species (gastropods *Limnaea* sp., *Gyraulus* sp. and *M. tuberculata*, pelecypod *Corbicula fluminalis*). In contrast to the previously described sequences M3 and M12, the latter low-brackish species are predominant. The upper part of the layer presents mycelium-like gypsum (Fig. 4D), as already described in unit G of section M3. Amphibious gastropods were also

found. Shell samples taken at the base of the unit yielded an age of 1270–1389 cal. AD.

Unit D is a grayish to brownish clayey silt. The unit presents a finely laminated structure, composed of light and dark layers. Some isolated layers are composed of sands and shell debris. Associated fauna is similar to those in unit C, as it comprises both lagoonal to slightly brackish species, but with a lower species diversity.

Unit E is a grayish to brownish sandy silt. It is a heterogeneous deposit, comprising shelly clayey-silt and sand layers (Fig. 4E). Clayey-silt layers are rich in *C. glaucum*. In some layers, clayey silt sediments form balls that are 2–5 mm in diameter. Some fine layers comprise pure and well-sorted shell fragments or sands. Centimeter-scale blocs from unit D have formed load structures upon finer layers (Fig. 4E). Finally, this unit comprises all the species observed in other units. The present shores of Maryut lagoon near point M4 were fixed between 1950 and 1970 (Awad, 2010) and mark the final sedimentation phase in this area.

4.4. Stratigraphy of core M14

Core M14 was taken near the El-Max canal that connects the Maryut to the sea (Fig. 1). The stratigraphy of core M14 displays just a single sedimentary unit, between 4 and 5.5 m bmsl deep, under a thick layer of human infill. It comprises evaporites alternating with organic-rich mud layers. Alternations occur at millimetric to centimetric scales. Halite grains are only present in the coarse sand fraction (>500 μm). They constitute large cubes and are totally transparent, between 0.5 and 5 mm large. Some are aggregated (Fig. 4F). The coarse sand fraction also comprises well-rounded

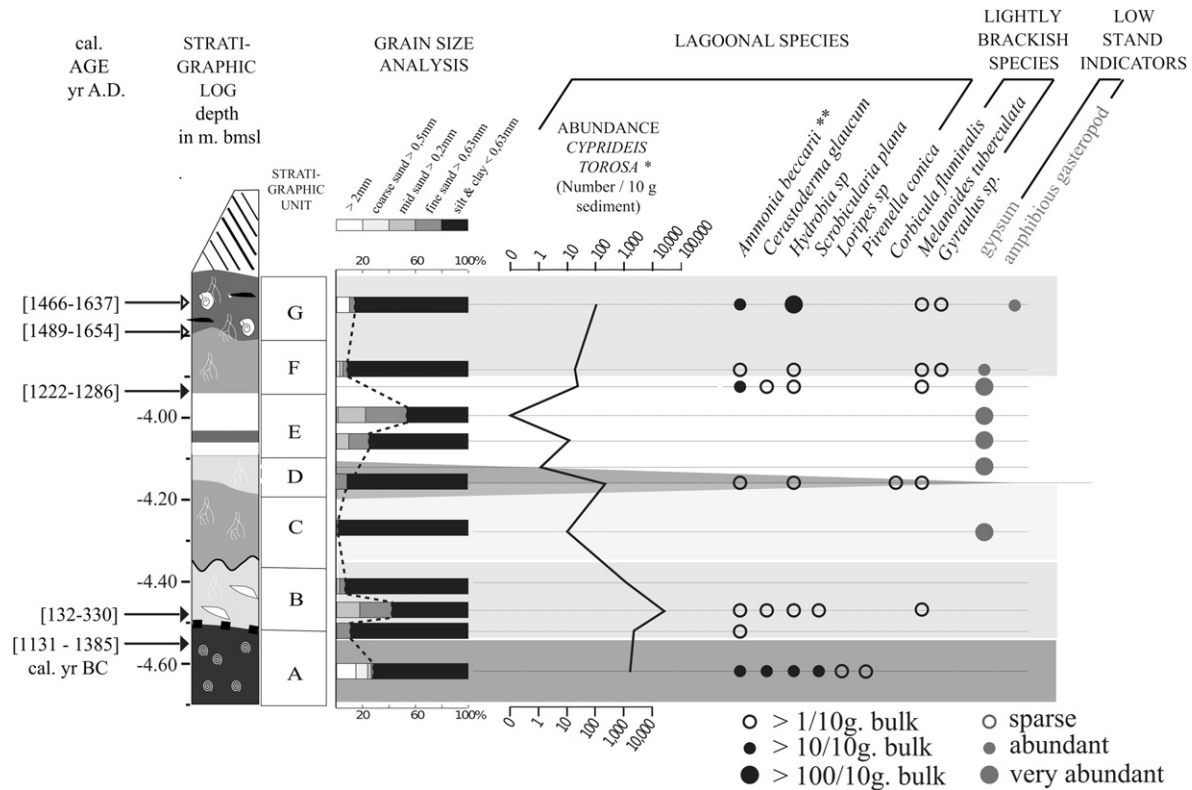


Fig. 3. Grain size analyses, macrofauna, *ostracoda, and **foraminifera data of stratigraphic log M3. Gypsum relative abundance and presence of amphibious gastropod shells are also shown. The facies legend is defined in Fig. 2.

carbonate grains. In the fine sand fraction (<200 μm), X-ray analysis yielded the following composition: ~80% gypsum, ~10% calcite and ~10% quartz. Gypsum crystals are transparent, generally automorph to sub-automorph and present prismatic morphologies with pyramidal terminations (Fig. 4G). Calcite corresponds to cylindrical peloids (Fig. 4G). No shells were recorded in this deposit. A hard crust (likely halite) stopped coring. Dating of an organic layer at the base of the sequence yielded an age of 1024–1156 cal. AD.

5. Hydrological changes inferred from the lagoon's bio-sedimentary record (Fig. 7)

5.1. Reservoir age

Goodfriend and Stanley (1996) elucidated in the present Maryut waterbody a hardwater radiocarbon effect (HWRE), which refers to the dilution of ^{14}C activity in the waterbody by the continental influx of ^{14}C -free inorganic carbon. These authors measured the radiocarbon age of a *Corbicula* shell, collected live at Alexandria in 1927. As results indicated an apparent age of 730 ± 60 yr BP, they deduced a hardwater radiocarbon error of 610 ± 60 yr. HWRE can also be estimated using the apparent ^{14}C age of lagoonal shells or organic matter taken in the topmost part of the sequence. A radiocarbon age obtained for a shell of *Cerastoderma* taken in unit G from section M3 (Fig. 3) indicated an apparent age of 345 ± 30 yr (Table 1) while a thin organic layer ~10 cm below the *Cerastoderma* sample yielded a similar age of 300 ± 30 yr. These recent ages are coherent with the last stage of the Maryut sedimentary sequence, before it dried up in the last 18th century AD and was then reclaimed in the last 19th century AD (see below). In addition, a bulk sample rich in organic matter taken in the upper sequence of

core M12 gave a radiocarbon age of 250 ± 30 yr, while a wood samples taken 30 cm below yielded a close radiocarbon atmospheric age of 165 ± 30 yr (Table 1). In light of this, samples were not corrected for a hardwater effect. The hardwater effect detected by Goodfriend and Stanley for the 20th century may translate hydrological changes within the Maryut lagoon since the late 19th century. At this time, the marginal and nearly dry lagoon (see Section 5.5) was reconnected to the Nile via an irrigation network and the water level was artificially lowered to 2.8 m bmsl for land reclamation purposes (Bernard, 1970; Warne and Stanley, 1993; ALAMIM, 2007; Awad, 2010).

Furthermore, because we interpret the water budget of the Maryut lake for the sequence studied as being Nile-dominated, we did not apply a marine reservoir age correction.

5.2. Brackish lagoon, ~2nd–3rd to ~8–9th centuries cal. AD

A dark shelly mud facies was elucidated at the base of sequences M3 (Figs. 2 and 3), M12 (Fig. 5) and M4 (Fig. 6). This facies records a marine-influenced lagoon whose accretion ended ~1200 cal. BC (Flaux et al., 2011). Goodfriend and Stanley (1996) also reported dominant marine inputs for this biofacies on the basis of stable isotope analyses. Following this shelly facies, a new phase of sedimentation is recorded after the 2nd–3rd centuries cal. AD in section M3 (Unit B, Fig. 3) and after the 8th–9th centuries cal. AD in section M12. The sedimentary record thus presents a hiatus of ~1500 years in section M3 and ~2000 years in core M12. In section M3, the biofacies deposited after the sedimentary hiatus is characterized by the monospecific proliferation of *C. torosa*. This ostracod is a pioneer species characteristic of a rapidly changing environment (Carbonel, 1988; Frenzel and Boomer, 2005; Ruiz et al., 2005). Associated *sensu stricto* lagoonal macrofauna and

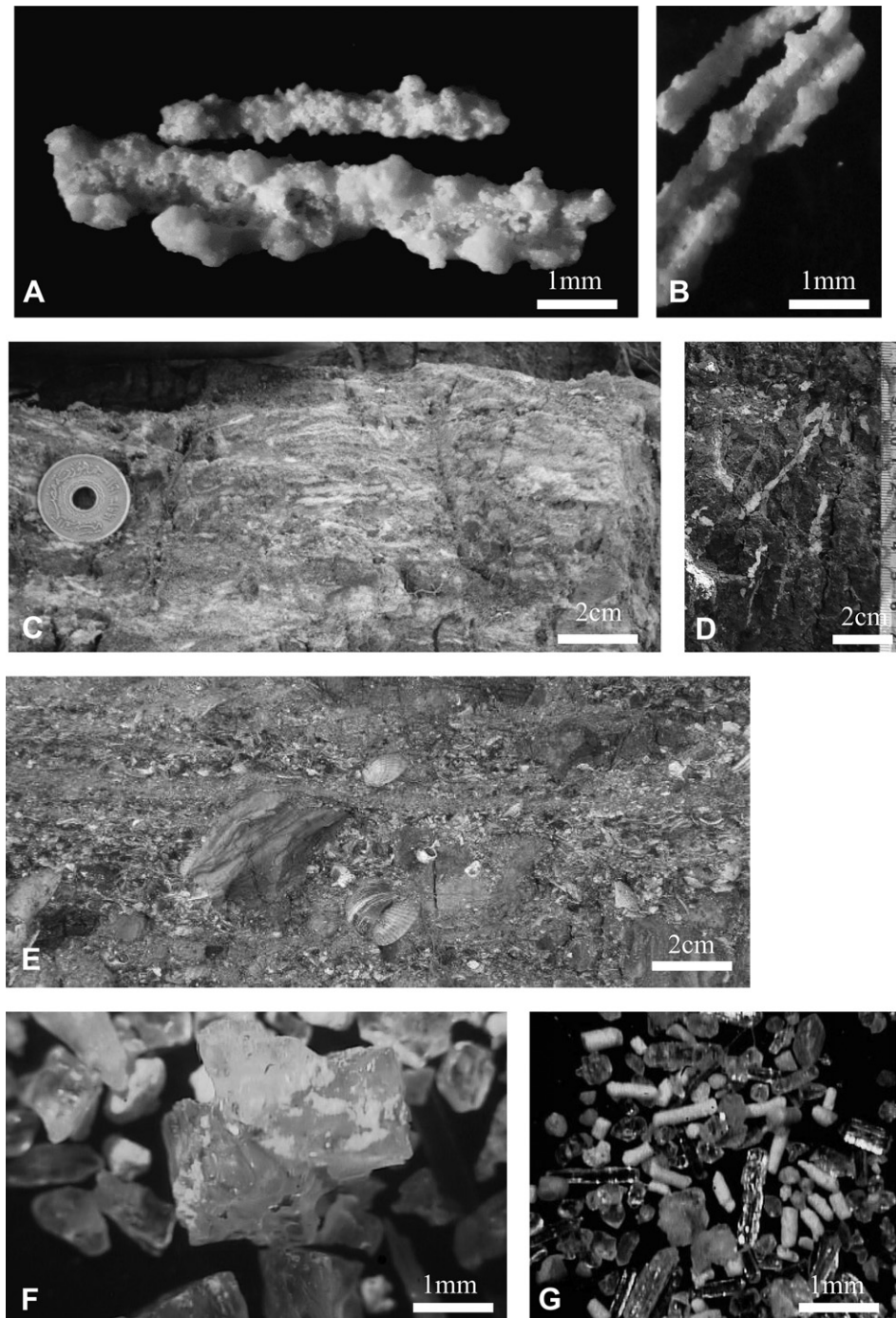


Fig. 4. Low water-level sedimentary features. (A) and (B): carbonate rhizoconcretions. Pedogenic feature interpreted as root influence on carbonate segregation (section M3, unit B); (C): millimetric to centrimetric bands of sandy gypsum and dark gray muds. The deposit was found ~4.0 m bmsl (section M3, unit E); (D): gypsum comprising a white silty sand, with mycelium-like structures (section M3, unit C). During fieldwork, this fine-grained gypsum was observed around the roots of living reeds; (E): fine heterogeneous layers in unit E, section M4. Note the pebble-size fragment from unit D (see Fig. 6) that forms a load cast upon fine layers; (F): Aggregated transparent halite cube from an evaporite layer in core M14; (G): sand fraction (between 0.2 and 0.5 mm) from an evaporite layer in core M14. Note transparent and prismatic gypsum crystals and white cylindrical peloids, probably produced by the crustacean *Artemia*.

brackish species attest to a lagoon environment with freshwater inputs (Fig. 3; Bernasconi and Stanley, 1994; Flaux et al., 2011). A similar mixed biofacies was elucidated in unit B of sequence M12 (Fig. 5). *C. tomentosa* and *C. zeylanica* found in the latter unit translate a lightly brackish setting (Corillion and Guerlesquin, 1971; Soulié-Märsche, 1999). They are associated with the euryhaline species *C. glaucum* and *S. plana*. The mixed faunal assemblages

attest to two water sources, oscillating between marine and Nile dominating inputs. This may imply a seasonal variation comprising, for example, a flood season with high freshwater inputs and a dry season subject to greater marine influence. Organic matter deposited in M12's biofacies has been dated to 694–894 cal. AD (Fig. 5). This phase therefore lasted from the ~2nd–3rd centuries cal. AD up to at least the ~8–9th centuries cal. AD (Fig. 7).

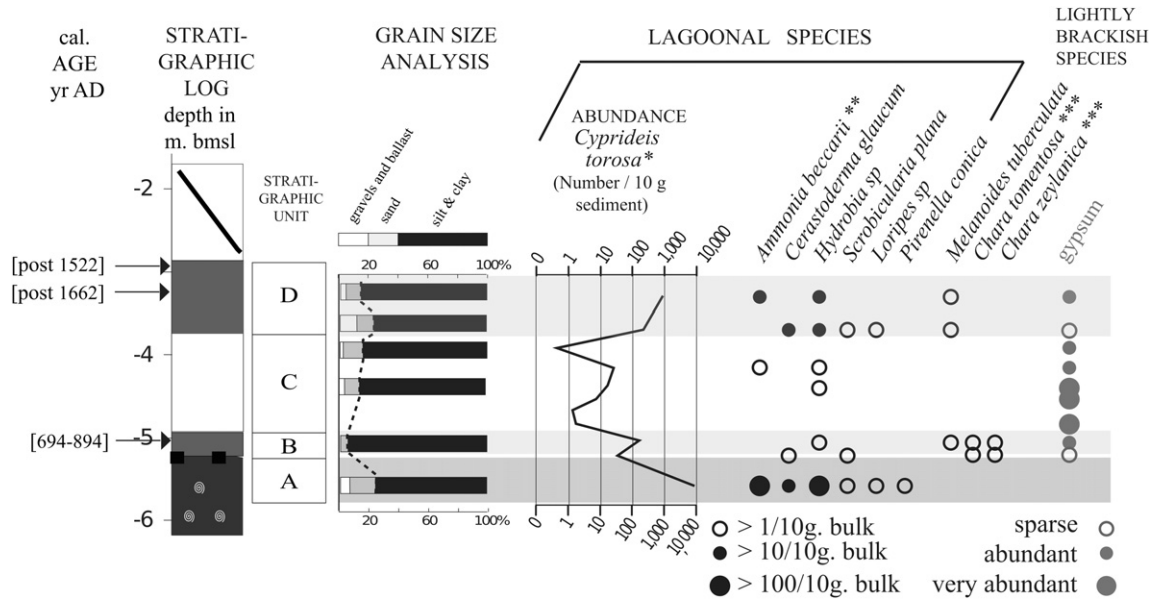


Fig. 5. Grain size analyses, macrofauna, *ostracoda, **foraminifera and ***characeae data of stratigraphic log M12. Relative abundances of gypsum are also shown. The facies legend is defined in Fig. 2, except unit C. It is a rich-gypsum deposit, but no gypsum-mud alternations were observed as in section M3, unit E.

5.3. Dessication between ~9–10th and ~13th centuries cal. AD

Rhizoconcretions (Fig. 4A and B) and the gasteropod *Gyraulus* sp. form sandy lenses in unit B of core M3 (Fig. 2). They are characteristic of brackish marsh shorelines (Bown, 1982; Plaziat and Younis, 2005; Mateucci et al., 2007). Mycelium-like gypsum deposits were also found (Figs. 2 and 4D). We assume that these

were formed from precipitation in pore water by evapo-transpiration processes, such as the gypsum concretions observed around root systems. Mycelium-like gypsum could thus reflect the presence of reed vegetation on the marsh shoreline. Moreover, the interface between units B and C is irregular (Fig. 2), consistent with an erosive surface. Such post-depositional features fit tightly with a phase of lower water levels. Gypsum formed in unit B of core M12

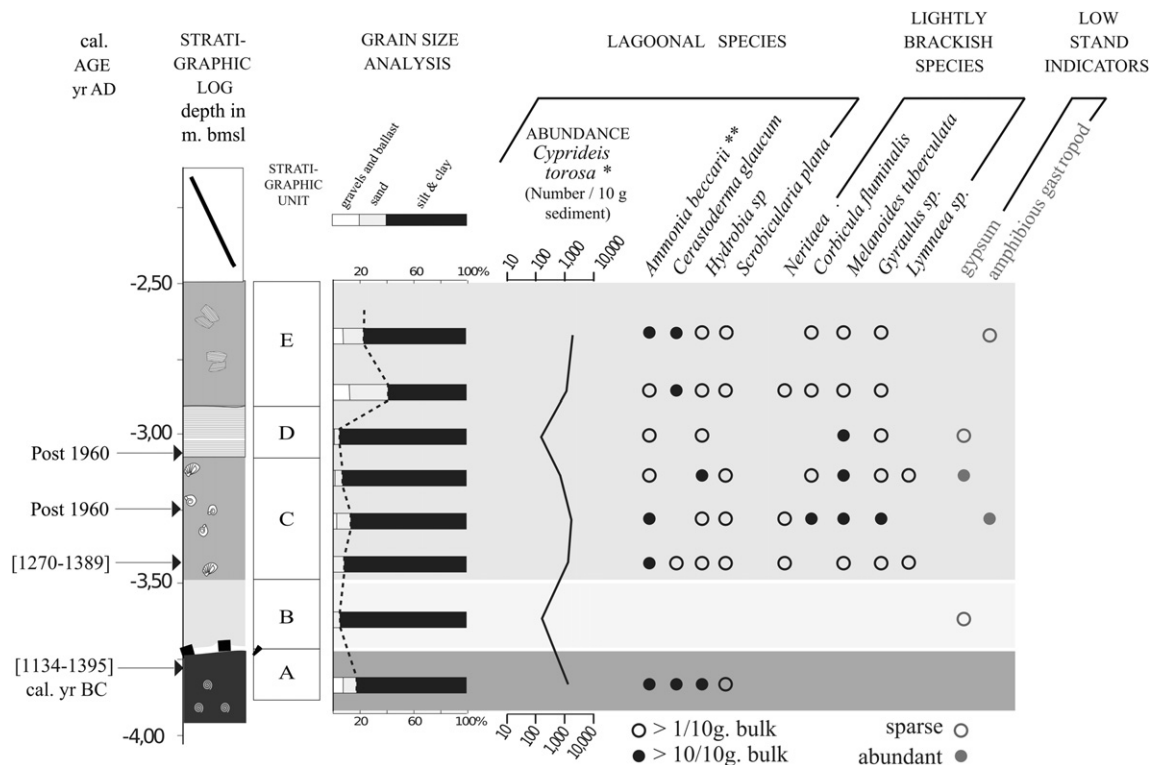


Fig. 6. Grain size analyses, macrofauna, *ostracoda, and **foraminifera data of stratigraphic log M4. Relative abundances of gypsum and the presence of amphibious gastropod shell are also shown. The facies legend is defined in Fig. 2, except for unit D: laminated structure.

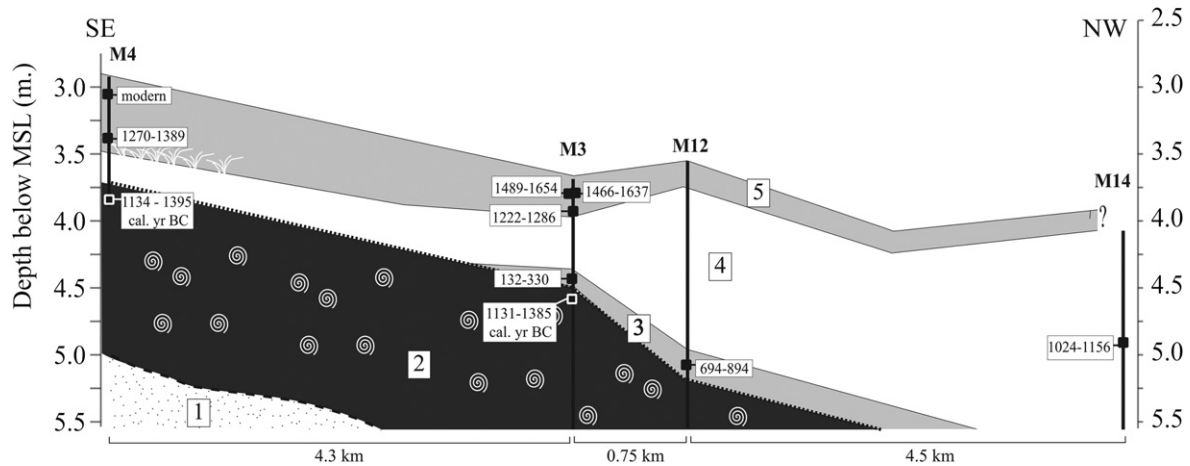


Fig. 7. Stratigraphic cross section constructed from cores M12 and M14 and sections M3 and M4. Numbers refer to the interpreted depositional environments: (1) late Pleistocene playa (Chen and Stanley, 1993); (2) marine influenced lagoon (Flaux et al., 2011); (3) brackish lagoon with important periodic freshwater inputs; (4) sebkhah; (5) brackish lagoon with important periodic freshwater input. Calibrated dates AD and sample depths are shown.

(Fig. 5) and unit B of section M4 (Fig. 6). In the latter, scarce *C. torosa* is the only faunal species recorded. A similar quasi-azoic facies is observed in unit C of section M3 (Fig. 3). According to Guelorget and Perthuisot (1983), who studied numerous marginal marine environments around the Mediterranean, such a low-diversity biocenosis with evaporitic minerals translates the confinement of the waterbody.

In section M3, the following unit D attests to evaporitic conditions, with high gypsum content (Fig. 3), as in unit C of core M12 (Fig. 5). The elucidated crystalline morphologies are known to form within freshly deposited organic-rich clayey sediments. In core M14, transparent and aggregated salt cubes indicate that they were formed within the water column and accumulated on the bottom of the basin to form a salt crust. Cylindrical calcite peloids (Fig. 4G) may be faecal pellets produced by the crustacean *Artemia*, well documented in hyperhaline environments (Schreiber, 1988; Elloumi et al., 2009). Well-defined gypsum-mud alternations (section M3, unit E, Fig. 4C) indicate, however, an oscillation between an evaporitic hydrological budget and silt inputs during Nile flooding. Alternation between salt crust and organic-rich mud deposits were also observed in core M14 and confirm the variability of the Maryut's water budget. Moreover, desiccation cracks observed in section M3 (Fig. 2, unit E) indicate that this lowstand ends by the emersion of the area around M3. At this time, the lagoon level was thus <4 m bmsl. Sediments from this phase record high gypsum content in the central basin (M3), while salt crystals were observed near Maryut shores (M14, Fig. 1). We first hypothesized that this gypsum-salt transect, from the central basin to its margin, translated a gradual increase in total dissolved salt in a shallow lagoon context. However, similar salt formations were not observed along other shores of this palaeo-sebkha. Of note, the core M14, characterized by intercalations of salt crusts and organic layers, is situated very close to the present El-Mexx canal, an outlet of the Maryut lagoon into the Mediterranean. This canal is attested in historical sources dating back to the 16th to 18th centuries AD (see Section 5.5). We suggest that core M14 may record a man-made saltmarsh, receiving seawater input via the El-Mexx canal. This period of negative water budget in the Maryut lagoon is recorded at least since 1024–1156 cal. AD (dating from core M14) up to 1222–1280 cal. AD (base of unit F, section M3, Fig. 3). Nonetheless, confinement processes may have begun earlier, after 694–894 cal. AD, as shown in core M12 (Fig. 7).

5.4. Brackish lagoon, ~13th to ~16th cal. centuries AD

After the deposition of the gypsum-rich facies in section M3, faunal groups from units F and G record a mixed assemblage, indicating euryhaline to lightly brackish conditions (Fig. 3). Similar biofacies from units C and D are recorded in M4 beginning around 1222–1280 cal. AD (Fig. 6) and can therefore be correlated with the post-gypsum units in M3 (Fig. 7). Although the faunal association from units C and D in M4 is very similar to M3's lagoonal biofacies, slightly brackish still water species predominate. This could reflect the proximity of M4 to Nile flow input through canals and important dilution of lagoon water by freshwater input, probably during seasonal floods or multi-annual periods of high river discharge. This phase indicates a perennial reconnection of the lagoon with the Nile, after the dessication phase.

5.5. Second drying-up phase, ~16th to ~18th centuries AD

Amphibious gastropods and mycelium-like gypsum found near the top of the sequence at sites M3 and M4, as well as organic-rich (peat-like) layer at site M3, attest to the proximity of the shoreline. High abundance of the gastropods *Hydrobia* sp. and *Gyraulus* sp. in the coarse sand fraction (Fig. 3) may result from sorting processes and accumulation at the shoreline by swell dynamics, because these shells have high floating ability. The upper sequence at site M3 has thus recorded shoreline changes, that are also attested in historical sources. Indeed, between the 16th and the 18th centuries AD, traveler accounts describe significant environmental changes in the Maryut basin (Sennoune, 2008). For example, during the summer 1663, Edward Melton explains that salt could be extracted from the 'Sebaka lake' (namely a sebkhah). The following February, Jean de Thévenot describes a 'marsh that stretches out as far as the eye can see'. During the winter of 1665, Antonio Gonzales writes of a 'lake as large as a sea'. These examples describe respectively three dominant landscapes: (1) a sebkhah, (2) a marshland, and (3) a vast lake. The different names attributed to the basin also attest to the variability of the lacustrine landscape, including *buchaira* (lake), *palus* (marsh) and *sebaca* (sebkhah). Moreover, four travelers describe a connection between the Maryut and the sea, near the current el-Maxx canal (Fig. 1). If this account is true, the basin became a vast lagoon around 40 km long, stretching from Alexandria to its southern shores (see the 0 msl contour line in Fig. 1). We compiled forty descriptions dated between the ~16th and ~18th

centuries AD and quantified the proportion of these four environments (lake, lagoon, marsh, sebkha), calculated over a period of 50 years. Results are depicted in Fig. 8A. Despite the annual to multi-annual scale variability in the water budget, the travelers' descriptions ($n = 40$) suggest a second desiccation of the lagoon during the 17th and the 18th centuries AD, characterized by a shoreline regression and a sebkha-like landscape (Fig. 8).

5.6. Maryut changes during the 19th–20th centuries

Goodfriend and Stanley (1996) have suggested that 2 m of sediments in core S79 (see location in Fig. 1) were deposited during the 20th century A.D. They attribute this very high sedimentation rate (19 mm yr^{-1}) to agricultural activities in the region and high supply of sediments from the lagoon margins and canals. Numerous amino acid racemization dates from shells in this layer indicate that the sediments have been significantly reworked (Goodfriend and Stanley, 1996). Unit E from section M4, dug near core S79, comprises abundant *C. glaucum* probably from unit A, while slightly brackish to freshwater species may be reworked from units C and D (Fig. 6). The facies also recovered well-sorted shell

debris layer. Clayey silt sediment balls were also found in this unit, as well as fragments from the underlying laminated unit D, that form load coats upon finer layers (Fig. 4E). These elements indicate a reworking lacustrine sediments by stream flow. The upper part of section M4 and core S79, located near the lagoon shoreline that was fixed between 1950 and 1970 (Awad, 2010). A thick layer of artificial fill was also elucidated in M3, M12 and M14. It is consistent with an extensive modification of the area by human activity (Awad, 2010).

6. Geoarchaeology of the Maryut

The environmental evolution of Maryut lagoon with regard to climatic (Nile flow), geomorphological (Canopic branch silting up) and delta land-use changes during the past 2000 years are discussed below and depicted in Fig. 8.

6.1. Maryut changes vs Nile flow

In 380 AD, Sozomen would have described dramatic flooding of the Maryut region by the Nile (cf. Goiran, 2001). Recent archaeological surveys suggest that most archaeological sites on the

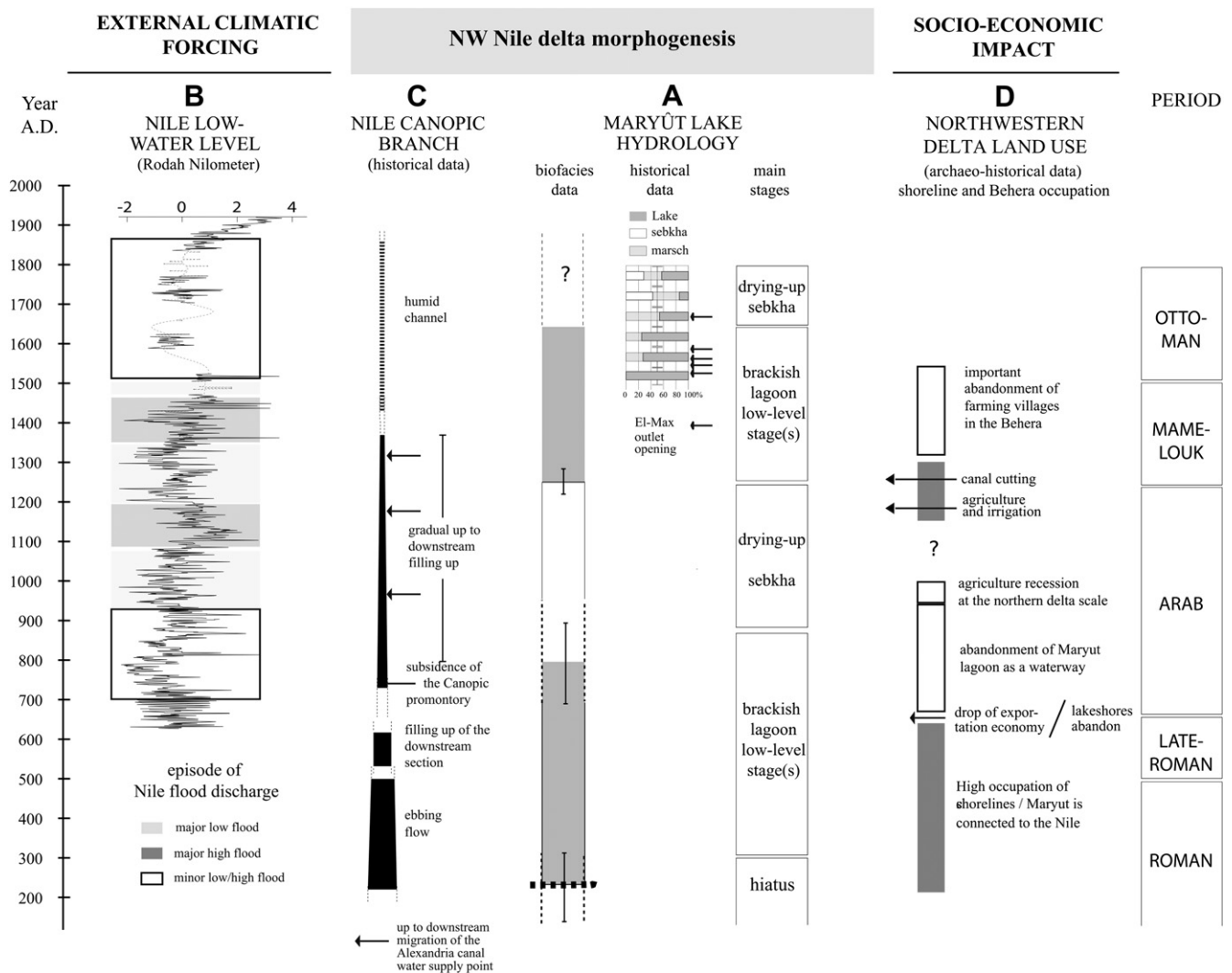


Fig. 8. (A) Synthesis of the Maryut's hydrological evolution between the 3rd and the 18th centuries AD as based on bio-sedimentary data, radiocarbon dates and historical evidence. This is depicted alongside (B) the Nile's low water level (Kondrashov et al., 2005; the time series have been centered on the relevant mean and the amplitudes have been normalized using the standard deviation of the original time series) and episode of Nile flood discharge (Hassan, 2007), (C) the Canopic branch's filling-up trend (references in text, Section 6.2), and (D) important economic and political changes (references in text, Section 6.3).

southeastern shores of the Maryut lagoon were built upon low mounds, just above mean flood level (Wilson, 2010). It is likely that seasonal flooding has been a major control of the Maryut's water budget. Annual Nile flow and flood data dating back to the 7th century AD have been gathered from the Nilometer at Rodah (Toussoun, 1925) in Cairo and corrected for Nile channel accretion by Popper (1951). Hassan (2007) highlights decadal-scale variations in Nile flow between the 9th and the 15th centuries AD (Fig. 8). Nile gauge records reveal pronounced episodes of low and high Nile flood discharge. Between 930 and 1070 AD, the Rodah Nilometer records both low flow and floods. This phase may have favored the first desiccation phase of the Maryut lagoon. However, between 1070 and 1200 AD, high Nile floods are archived while a negative water budget is recorded in the Maryut lagoon. At this centennial timescale, Nile flow does not appear to be a major driver of Maryut changes. Nonetheless, seasonal fluctuation of Nile flooding is obviously key in shaping rapid Maryut changes, as depicted by travelers from the 16th to the 18th centuries AD (Fig. 8). The southeastern part of the Maryut basin, whose a vast surface lies between -2 and 0 m below msl, would have been particularly sensitive to phases of emersion and flooding. It suggests a rapidly fluctuating shoreline position which was not favorable to human occupation. Indeed, there are no archaeological evidences such as harbors features for occupation of the Maryut shores during the Medieval period.

6.2. Water deviation and canopic branch decline

The Canopic was formerly the westernmost branch of the Nile delta (Fig. 1). Alexandria and its hinterland were dependent upon this branch for freshwater supplies. According to Toussoun (1922, 1926), the Canopic's flow began to ebb between the 1st and the 5th centuries AD. During this period, Chen et al. (1992) note the rapid progradation of the Rosetta lobe, probably to the detriment of the Canopic branch. Bernand (1970) suggests that flow diminished from the 2nd century AD onwards and that the mouth had already silted up by the 5th century AD. Toussoun (1926) found no references to the Canopic branch in Arabic texts. The important city of Naukratis, located on the banks of the Canopic channel, ceased to exist in the early 8th century AD (Coulson, 1996). Hairy and Sennoune (2006) have used historical sources to show how the layout of Alexandria's canal system evolved as the Canopic gradually silted up during the medieval period, especially between the 10th and the 14th centuries AD. This chronology is contemporaneous with the first desiccation phase of the Maryut described in the present study. Bernand (1970) has suggested that a decline in Canopic flow began during Roman time when Alexandria's demands for freshwater were growing rapidly. In addition, Canopic flow was diverted, via numerous canals, into the Maryut. In the same manner, Blouin (2006) used papyrus documents to demonstrate that flow in the Mendesian branch of the eastern delta declined during the 2nd century AD, in response to the irrigation network and canals. The irrigation and freshwater supply systems of Alexandria and its countryside may therefore be one of the causes behind a decrease in Canopic flow. We suggest that an increasing freshwater demand led to the deviation of Canopic water and the silting up of its channel. At this millennial timescale, the increasing diversion of Nile flow by societies since antiquity probably induced the disappearance of five of the seven branches known in ancient times (Toussoun, 1922).

6.3. The Maryut's environmental history in relation to historical evidence of navigation and delta irrigation

During antiquity, Maryut lagoon served as a navigable waterway linking Alexandria with the delta (Rodziewicz, 1998; Empereur,

1998). Historical evidence (Yoyotte et al., 1997), archaeological data (Wilson, 2010) and sedimentological studies (Toonen and Trampier, 2010) suggest that the Maryut, known as *Lake Mareotis* in antiquity, was supplied with freshwater from the Nile via branches and/or canals. Our data partially confirm these conclusions, because biofacies between the 2nd–3rd and the 8–9th centuries cal. AD are consistent with fluvial input into the lagoon (Fig. 7). Flaux et al. (2011) have demonstrated that the Maryut was a marine influenced lagoon at least until the 11–12th centuries cal. BC (corresponding to the shelly facies, see Figs. 3, 5 and 6). Although the sedimentary hiatus in our record does not allow us to document the rate of evolution from a marine to fluvial dominated lagoon, this environmental change may indicate human impacts, contemporaneous with the development of Alexandria, its lacustrine navigation routes (Wilson, 2010) and agricultural hinterland during antiquity (Redon, 2007, p. 450–458).

From the 7th to the 9th centuries AD, important political changes took place in the Nile delta. Persian invasions occurred in 619 AD. After the Arab conquest (639–642 AD), the export economy of Alexandria's countryside declined and nearly all of the Maryut's sites were abandoned (Empereur, 1998; Rodziewicz, 1998; Wilson, 2010; Blue and Khalil, in press). The role of Maryut lagoon as an important transport interface declined and fluvial waterways were slowly abandoned (Décobert, 2002). During the 9th century AD, the construction of a new city wall around Alexandria separated the urban area from its lacustrine façade (Haas, 2001). Shortland et al. (2006) list a series of political disorders, rebellions and revolts in the western delta region during the 8th and 9th centuries AD, as well as Berber incursions from the Libyan Desert in the 9th century AD. Finally, Toussoun (1922), quoting a 10th century AD Arab writer, describes a major decrease of the northern delta's agricultural base, which he attributes to poorly maintained irrigation canals. We suggest that political disruptions and socio-economic changes between the 7th and 9th centuries AD were key drivers of Maryut desiccation during the 9–10th centuries AD (Fig. 8).

Guest (1912) suggested that canal networks in the delta were significantly modified during the 12th century AD. Toussoun (1926), based on Arabic chronicles, indicated that the Behera channel was dredged between 1263 and 1265 at time of the Mamluk Sultan al-Zahir Baybars. We suggest that higher Nile water supply (as related to the Rosetta branch), linked to the development of an irrigation system, ended the Maryut's negative water budget during the 13th century cal. AD (Fig. 8).

Michel (2002) studied two tax records dating at 1315 and 1528, drawing up a list of farming villages and their associated lands in the Behera. Between these two dates, the author shows, from a sample of fifty-one villages, that eight are deserted and sixteen are significantly depopulated, while the cultivated acreage is halved. This decline is not specific to the region. It is attributed to a major demographic crisis induced by a plague that ravaged the population during this period. More specifically, however, the small size of the Behera villages (and their associated cultivated lands) and their location at the delta margin were probably also significant in shaping the decline of the area. Within the Behera itself, the western part was the most affected. Michel (2002) adds that in the early years of the Ottoman period, emigration took place from the Nile delta margins toward the center. Thus, from the 14th to the 16th centuries AD, the population of the Behera region decreased significantly. Subsequently, it is assumed that the hydrological system of the Behera was at least partially abandoned, especially in its western part. The hydrological regime of the Maryut lagoon was directly affected by the demographic and agricultural decline of the Behera, as is confirmed by our data with the second desiccation phase of the basin during the 17th century AD (Fig. 7). As a consequence, when the French Expedition reached Egypt between 1798

and 1801, engineers described the Maryut as a barren sandy salt-marsh, called sebâkhah by local inhabitants.

7. Conclusion

Study of the sedimentary record of the Maryut lagoon served to refine interpretations of the Maryut environmental history from the 2nd to the 18th centuries AD. Sedimentological, paleontological and historical data allow us to identify four major environmental periods. The Maryut's water budget oscillated between a fluvial-dominated euryhaline lagoon regime (2nd–3rd to 8–9th and 13th to 16th centuries cal. AD) and that of a periodically flooded sebkhah (9–10th to 13th and 17th–18th centuries cal. AD). Based on comparisons with land use history, we propose that political and socio-economical disruptions between the 7th and 9th centuries AD, and an important decrease in population during the 14th to 16th centuries AD, both led to a negative water budget in the Maryut lagoon, as a result of a reduction of irrigation water inputs. Drying-up phases are consistent with periods of abandonment of the Behera region. Conversely, we propose that irrigation works in the area in the 13th century AD induced the end of evaporitic conditions. At the end of the 19th century AD, the Maryut basin once again became artificially connected to the Nile via the northwestern delta's expanding irrigation network (Awad, 2010). Changes in human occupation were probably superimposed on the long-term recession of the western delta margin, in response to silting-up of the Canopic branch. This process might have resulted, at least in part, from the diversion of Canopic flow into the irrigation system. The environmental history of the Maryut lagoon during the past 2000 years therefore reflects the economic dynamics of the Alexandrian region. A finer temporal and spatial resolution of the Maryut's sedimentary record will help to better understand seasonal to annual Nile flow variability and its impact on the basin's water budget, human occupation and agricultural dynamics.

Acknowledgments

This study was supported by the French National Research Agency (ANR): project PALEOMED. The ARTEMIS-INSU program financed ¹⁴C dates. Financial support for exchanges between Egyptian and French researchers was provided by the IMHOTEP program (Hubert-Curien partnership). The authors also thank the CEAlex (CNRS – USR 3134, head J.-Y. Empereur) and its topographic service for technical and logistic help during fieldwork. We thank anonymous reviewers for fruitful comments on an earlier version of the paper.

References

- ALAMIM project, 2007. Alexandria Lake Maryut Integrated Management, Alexandria, Egypt, Stocktaking Analysis (a), Background Material. Workshop Internal Report, Alexandria, <http://smap.ew.eea.europa.eu/foi120392/prj885304/>.
- Awad, I., 2010. A study of the evolution of the Maryut Lake through maps. In: Blue, L., Khalil, E. (Eds.), Lake Mareotis: Reconstructing the Past, Proceedings of the International Conference on the Archaeology of the Mareotic Region Held at Alexandria University, Egypt 5th–6th April 2008. University of Southampton Series in Archaeology, vol. 2. BAR 52113, Oxford, pp. 11–33.
- Bernard, A., 1970. Le delta Egyptien d'après les textes grecs. 1 – les confins Libyques. IFAO, Le Caire.
- Bernasconi, M.P., Stanley, D.J., 1994. Molluscan biofacies and their environmental implications, Nile delta lagoons, Egypt. *Journal of Coastal Research* 10 (2), 440–465.
- Blouin, K., 2006. Homme et milieu dans le nome mendésien à l'époque romaine (1er au 6e S.). PhD thesis, University of Nice Sophia Antipolis, France and University of Laval, Québec, 558 pp.
- Blue, L., Khalil, E. (Eds.), 2010. Lake Mareotis: Reconstructing the Past. Proceedings of the International Conference on the Archaeology of the Mareotic Region Held at Alexandria University, Egypt, 5th–6th April 2008. University of Southampton Series in Archaeology, vol. 2. Bar International Series 2113, Oxford, p. 156.
- Blue, L., Khalil, E., Trakadas, A. (Eds.), 2011. A Multidisciplinary Approach to Alexandria's Economic Past: The Lake Mareotis Research Project. University of Southampton Series in Archaeology, vol. 5. Bar International Series 2285, Oxford, p. 313.
- Bown, T.M., 1982. Ichnofossils and rhizoliths of the nearshore fluvial jebel Qatrani formation (oligocène), Fayum province, Egypt. *Palaeogeography, Palaeoclimatology, Palaeoecology* 40, 255–309.
- Carbonel, P., 1988. Ostracods and the transition between fresh and saline waters. In: De Dekker, P., Colin, J.-P., Peypouquet, J.-P. (Eds.), *Ostracoda in the Earth Sciences*. Elsevier Science Publishers, Amsterdam, pp. 157–174.
- Chen, Z., Warne, A.G., Stanley, J.D., 1992. Late quaternary evolution of the north-western Nile Delta between the Rosetta promontory and Alexandria, Egypt. *Journal of Coastal Research* 8 (3), 527–561.
- Chen, Z., Stanley, D.J., 1993. Alluvial stiff muds (late Pleistocene) underlying the lower Nile delta plain, Egypt: petrology, stratigraphy and origin. *Journal of Coastal Research* 9 (2), 539–576.
- Corillon, J., Guerlesquin, M., 1971. Notes phytogéographiques sur les Charophycées d'Égypte. *Revue Algologique* 2, 178–191.
- Cosson (de), A., 1935. Mareotis, Being a Short Account of the History of Ancient Monuments of the North-western Desert of Egypt and of Lake Mareotis. Country Life Ltd, London.
- Coulson, W.D.E., 1996. Ancient Naukratis. In: *Oxbow Monographs* 60. Oxford.
- Décobert, C., 2002. Maréotide médiévale. Des bédouins et des chrétiens. In: Décobert, C. (Ed.), *Études Alexandrines* 8, Alexandrie Médiévale, vol. 2. IFAO, Le Caire, pp. 127–167.
- El Asmar, H.M., Wood, P., 2000. Quaternary shoreline development: the north-western coast of Egypt. *Quaternary Science Reviews* 19, 1137–1149.
- Elloumi, J., Carrias, J.-F., Ayadi, H., Sime-Ngando, T., Bouaïn, A., 2009. Communities structure of the planktonic halophiles in the solar saltern of Sfax, Tunisia. *Estuarine, Coastal and Shelf Science* 81, 19–26.
- Empereur, J.-Y., 1998. Alexandrie redécouverte. Fayard, Paris.
- Empereur, J.-Y., Picon, M., 1998. Les ateliers d'amphores du lac Mariout. In: Empereur, J.-Y. (Ed.), *Commerce et artisanat dans l'Alexandrie hellénistique et romaine*, Athènes 11–12 décembre 1998. *Bulletin de correspondance Hellénique*, pp. 75–91.
- Flaux, C., Morhange, C., Marriner, N., Rouchy, J.-M., 2011. Bilan hydrologique et biosédimentaire de la lagune du Maryût (delta du Nil, Égypte) entre 8000 et 3200 ans cal. B.P. *Géomorphologie: relief, processus et environnement* 3, 261–278.
- Frenzel, P., Boomer, I., 2005. The use of ostracods from marginal marine, brackish waters as bioindicators of modern and Quaternary environmental changes. *Palaeogeography, Palaeoclimatology, Palaeoecology* 225, 68–92.
- Goiran, J.-P., 2001. Recherches géomorphologiques dans la région littorale d'Alexandrie en Égypte. PhD thesis in physical geography, Université de Provence, Aix-Marseille, 264 pp.
- Goiran, J.-P., Marriner, N., Morhange, C., Abd el-Maguid, M., Espic, K., Bourcier, M., Carbonel, P., 2005. Evolution géomorphologique de la façade maritime d'Alexandrie (Égypte) au cours des six derniers millénaires. *Méditerranée* 104, 61–65.
- Goodfriend, G.A., Stanley, D.J., 1996. Reworking and discontinuities in Holocene sedimentation in the Nile Delta: documentation from amino acid racemization and stable isotopes in mollusks shells. *Marine Geology* 129, 271–283.
- Guelorget, O., Perthuisot, J.P., 1983. Le domaine paraliq. Expressions géologiques, biologiques et économiques du confinement. In: *Travaux du laboratoire de Géologie, Ecole Normale Supérieure Paris*, 16, 1–136.
- Guest, A.R., 1912. A note on the branches of the Nile and the Kurahs of lower Egypt, with map. *Journal of the Royal Asiatic Society of Great Britain and Ireland*, 941–980.
- Haas, C., 2001. Alexandria and the Mareotis region. In: Burns, Th.S., Eadie, J.W. (Eds.), *Urban Centers and Rural Contexts in Late Antiquity*, East Lansing, Michigan, pp. 47–62.
- Hairy, I., Sennoune, O., 2006. Géographie historique du canal d'Alexandrie. *Annales Islamologiques* 40, 247–278.
- Hassan, F.A., 2007. Extreme Nile floods and famines in Medieval Egypt (AD 930–1500) and their climatic implications. *Quaternary International* 173–174, 101–112.
- Khalil, E., 2005. Egypt and the Roman Maritime Trade, a Focus on Alexandria, Philosophy. PhD thesis, University of Southampton, 333 pp.
- Kondrashov, D., Feliks, Y., Ghil, M., 2005. Oscillatory modes of extended Nile river records (AD 622–1922). *Geophysical Research Letters* 32. <http://dx.doi.org/10.1029/2004GL022156>.
- Mateucci, R., Belluomini, G., Manfra, L., 2007. Late Holocene environmental change in the coastal Somalia inferred from Achatina and rhizoliths. *Journal of African Earth Sciences* 49 (3), 79–89.
- Michel, N., 2002. Villages désertés, terres en friche et reconstruction rurale en Égypte au début de l'époque Ottomane. *Annales Islamologiques* 36, 147–151.
- Plaziat, J.-C., Younis, W.R., 2005. The Modern Environments of Molluscs in Southern Mesopotamia, Iraq: a Guide to Paleogeographical Reconstructions of Quaternary Fluvial, Palustrine and Marine Deposits. *Carnets de Géologie, Brest*. <http://dx.doi.org/10.4267/2042/1453>.
- Popper, W., 1951. The Cairo Nilometer. University of California Press, Los Angeles.
- Redon, B., 2007. Le Delta égyptien aux temps des Grecs. La présence grecque en Basse Égypte, de l'époque saïte à la fin de l'époque hellénistique: diffusion, nature, intensité et conséquences. PhD thesis, Univ. Lille III, 605 pp.

- Reimer, P.J., Baillie, M.G.L., Bard, E., Bayliss, A., Beck, J.W., Blackwell, P.G., Bronk Ramsey, C., Buck, C.E., Burr, G.S., Edwards, R.L., Friedrich, M., Grootes, P.M., Guilderson, T.P., Hajdas, I., Heaton, T.J., Hogg, A.G., Hughen, K.A., Kaiser, K.F., Kromer, B., McCormac, F.G., Manning, S.W., Reimer, R.W., Richards, D.A., Southon, J.R., Talamo, S., Turney, C.S.M., Van der Plicht, J., Weyhenmeyer, C.E., 2009. IntCal09 and Marine09 radiocarbon age calibration curves, 0–50,000 years cal BP. *Radiocarbon* 51 (4), 1111–1150.
- Rodziewicz, M., 1998. From Alexandria to the West by land and by waterways. In: Empereur, J.-Y. (Ed.), *Commerce et artisanat dans l'Alexandrie hellénistique et romaine*, Athènes 11–12 décembre 1998. *Bulletin de correspondance Hellénique*, pp. 93–103.
- Ruiz, F., Abad, M., Bodergat, A.M., Carbonel, P., Rodriguez-Lazaro, J., Yasuhara, M., 2005. Marine and brackish-water ostracods as sentinels of anthropogenic impacts. *Earth-Science Reviews* 72, 1–2, 89–111.
- Senoune, O., 2008. *Alexandrie et les récits de voyageurs du 4ème siècle à 1798*. PhD thesis, University Lumière, Lyon 2, 993 pp.
- Schreiber, B.C., 1988. Subaqueous evaporite deposition. In: Schreiber, B.C. (Ed.), *Evaporites and Hydrocarbons*. Columbia University Press, pp. 182–255.
- Shortland, A., Schachner, L., Freestone, I., Tite, M., 2006. Natron as a flux in the early vitreous materials industry: sources, beginnings and reasons for decline. *Journal of Archaeological Science* 33, 521–530.
- Soulié-Marsche, I., 1999. Extant gyronite populations of *Chara zeylanica* and *C. haitensis*. *Australian Journal of Botany* 47/2, 371–382.
- Stanley, D.J., Goddio, F., Jorstad, T.F., Schnepf, G., 2004a. Submergence of ancient Greek cities off Egypt's Nile delta – a cautionary tale. *Geological Society of America* 14, 4–10.
- Stanley, J.D., Warne, A.G., Schnepf, G., 2004b. Geoarchaeological interpretation of the Canopic, largest of the relict Nile delta distributaries, Egypt. *Journal of Coastal Research* 20 (3), 920–930.
- Stanley, J.D., 2005. Growth faults, a distinct carbonate-siliciclastic interface and recent coastal evolution, NW Nile Delta, Egypt. *Journal of Coastal Research* 42, 309–318.
- Stanley, J.D., Jorstad, T.F., 2006. Short contribution: buried canopic channel identified near Egypt's Nile Delta coast with radar (SRTM) imagery. *Geoarchaeology* 21 (5), 503–514.
- Stanley, D.J., Toscano, M.A., 2009. Ancient archaeological sites buried and submerged along Egypt's Nile delta coast: gauges of Holocene delta margin subsidence. *Journal of Coastal Research* 25 (1), 158–170.
- Stuiver, M., Reimer, P.J., Reimer, R.W., 2005. CALIB 5.0. WWW Program and Documentation.
- Toonen, W.H.J., Trampier, J., 2010. The holocene Nile settlement dynamics in the western Nile delta. In: Tristan, Y., Ghilardi, M. (Eds.), *Landscape Archaeology. Egypt and the Mediterranean World*, International Colloquium on Geoarchaeology, Programme and Abstracts Volume, Cairo, 19–20 September, p. 116.
- Toussoun, O., 1922. Mémoires sur les anciennes branches du Nil, époque ancienne. In: *Mémoire de l'Institut d'Égypte*, vol. 4. IFAO, Le Caire.
- Toussoun, O., 1925. Mémoire sur l'histoire du Nil. In: *Mémoire de l'Institut d'Égypte*, vol. 18. IFAO, Le Caire, pp. 366–404.
- Toussoun, O., 1926. La géographie de l'Égypte à l'époque arabe, tome 1, partie 1. In: *Mémoire de la Société Royale Archéologique d'Alexandrie*, tome, vol. 8. IFAO, Le Caire.
- Warne, A.G., Stanley, D.J., 1993. Late Quaternary evolution of the northwest Nile delta and adjacent coast in the Alexandria region, Egypt. *Journal of Coastal Research* 9, 26–64.
- Wilson, P., 2010. Recent survey work in the southern Mareotis area. In: Blue, L. (Ed.), *Lake Mareotis: Reconstructing the Past*. Proceedings of the International Conference on the Archaeology of the Mareotic Region Held at Alexandria University, Egypt, 5th–6th April 2008. University of Southampton Series in Archaeology, vol. 2. Bar International Series 2113, Oxford, pp. 119–125.
- Woodward, J.C., Macklin, M.G., Krom, M.D., Williams, M.A.J., 2007. The Nile: evolution, quaternary river environments and material fluxes. In: Gupta, A. (Ed.), *Large Rivers: Geomorphology and Management*, pp. 261–292.
- Yoyotte, J., Charvet, P., Gompertz, S., 1997. *Strabon, le voyage en Égypte, un regard romain*. Nil Edition, Paris, 313 pp.